Self-heating study of an AlGaN/GaN-based heterostructure field-effect transistor using ultraviolet micro-Raman scattering

I. Ahmad, V. Kasisomayajula, and M. Holtz[a)]
Department of Physics, Texas Tech University, Lubbock, Texas 79409

J. M. Berg
Department of Mechanical Engineering, Texas Tech University, Lubbock, Texas 79409

S. R. Kurtz, C. P. Tigges, A. A. Allerman, and A. G. Baca
Sandia National Laboratory, Albuquerque, New Mexico 87185

(Received 22 December 2004; accepted 9 March 2005; published online 18 April 2005)

We report micro-Raman studies of self-heating in an AlGaN/GaN heterostructure field-effect transistor using below (visible 488.0 nm) and near (UV 363.8 nm) GaN band-gap excitation. The shallow penetration depth of the UV light allows us to measure temperature rise (ΔT) in the two-dimensional electron gas (2DEG) region of the device between drain and source. Visible light gives the average ΔT in the GaN layer, and that of the SiC substrate, at the same lateral position. Combined, we depth profile the self-heating. Measured ΔT in the 2DEG is consistently over twice the average GaN-layer value. Electrical and thermal transport properties are simulated. We identify a hotspot, located at the gate edge in the 2DEG, as the prevailing factor in the self-heating. © *2005 American Institute of Physics*. [DOI: 10.1063/1.1906305]

Wide band-gap semiconductor GaN has recently been used to develop heterostructure field effect transistors (HFETs) for high power and microwave applications.[1–4] The large piezoelectric and spontaneous polarization fields occurring in the AlGaN/GaN heterostructures generate a quasi-two-dimensional electron gas (2DEG) at the heterointerface without doping, and the 2DEG forms the conductive channel between the HFET drain and source (D–S). With the 2DEG confined within ≈10 nm and narrow HFET gate widths, channel current densities can be very high in these devices, leading to significant local Joule heating. This self-heating degrades HFET performance or results in irreversible damage. Thermal management is crucial to the viability of these devices, motivating accurate measurements of self-heating.

Figure 1 shows the $I-V$ characteristics of the device studied here; the inset to Fig. 1 depicts the device structure.[5] The $Al_{0.19}Ga_{0.81}N/GaN$ structure is grown on a 6H–SiC substrate. The device is composed of Ohmic source and drain contacts separated by 5 μm and a 2-μm-Schottky gate at the D–S center. The 1.5-μm-wide "windows" on each side of the gate are used for our micro-Raman measurements. The device gate width is 150 μm. We separate the $I-V$ dependence into below and above saturation regions, and demark them with vertical lines at the V_{D-S} values for each V_g. These two regions meet where a segment of the 2DEG has become depleted (with low carrier density and decreased mobility due to enhanced scattering) and drift velocity saturates.[6] Above this voltage (II) we see the current diminish with increasing V_{D-S}. This decrease correlates with the development of a localized "hotspot" at the gate edge, where the self-heating effect is strongest.

Self-heating effects in these devices can be studied using micro-Raman spectroscopy via shift in the phonon energy (E_2^2 for GaN).[7] To date, these have been performed solely using conventional visible excitation. Previous studies have exploited visible micro-Raman to laterally map self-heating in AlGaN/GaN HFETs.[8–10] Because GaN is transparent to visible light, one obtains an average measure of temperature limited by the layer thickness (or depth of focus), and the focus spot size. In contrast, micro-Raman measurements using near-band-gap ultraviolet (UV) excitation sample a shallow, near-surface region. For excitation wavelength 363.8 nm, the optical penetration depth is $d_{opt}<100$ nm in GaN,[11] close to the relevant length scale of the HFET active region and 2DEG. These measurements allow us to study the temperature rise (ΔT) of the HFET 2DEG region. We directly compare our results with micro-Raman measurements of the average ΔT in the GaN layer using sub-band-gap excitation (488.0 nm) under identical conditions. The visible measurements allow us to simultaneously obtain ΔT in the substrate via the SiC phonon shifts. Combined, the UV and visible studies provide us with a temperature depth profile of the structure under varying drive conditions, for which we

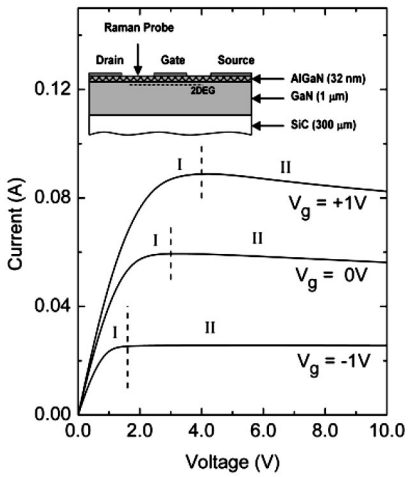

FIG. 1. $I-V$ dependence for the AlGaN/GaN HFET at different V_g. Inset: device layout (not to scale).

[a)]Electronic mail: mark.holtz@ttu.edu

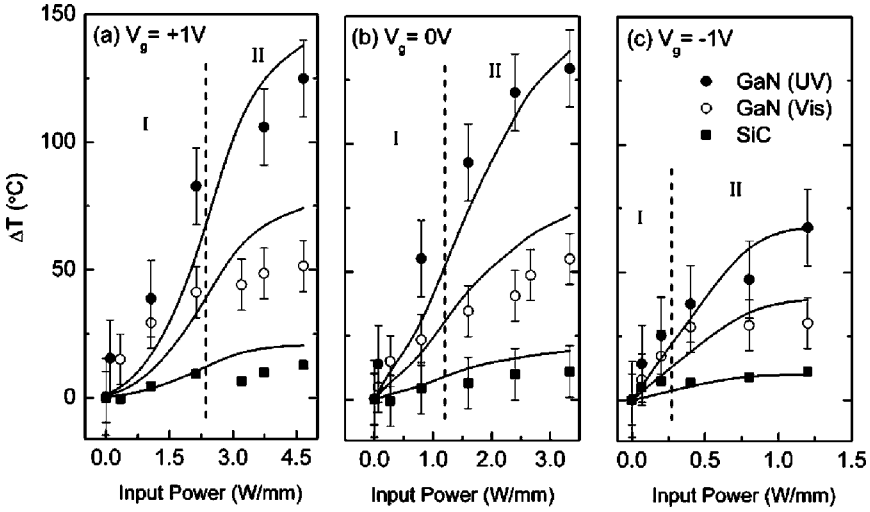

FIG. 2. Temperature rise (from ambient) vs. input power at gate voltages (a) +1 V, (b) 0 V, and (c) −1 V. 2DEG from UV Raman data (●). Average GaN (○) and SiC (■) from visible Raman data. Solid curves are simulation results.

find no previous report. We support our results with electrical and thermal simulations of the device.

Figure 2 shows measured temperature rise ΔT from room temperature versus input power for the same conditions as in Fig. 1. The measurements are performed $\sim 0.3\ \mu$m from the gate edge on the drain ($V \geqslant 0$) side; the focal spot is $\sim 0.6\ \mu$m in diameter. In each panel we show the GaN ΔT measurements using UV excitation, GaN with visible light, and SiC substrate temperature (visible). Values observed using UV light are consistently two to three times higher than those obtained with visible light due to the fact that the UV probe emphasizes the AlGaN/GaN interfacial region where the local Joule heating takes place. As expected, the lowest ΔT values in Fig. 2 are for the SiC substrate since it has good thermal conductivity and is attached to a heat sink. We note in each panel a relatively rapid rise in temperature followed by a somewhat slower rise with input power. Our overall thermal resistance from the visible Raman measurements is $10.4 \pm 1.8\ ^\circ\mathrm{C}/(\mathrm{W}/\mathrm{mm})$, in good agreement with previously reported results from similar devices.[10]

We have conducted combined electrical and thermal simulations of the device structure. Two approaches are used to simulate the electrical behavior. A 2D finite difference analysis[12] is used to self-consistently solve the Poisson equation coupled with the continuity and Schrödinger equations.[13] The FE analysis includes 1 μm thick GaN followed by the $Al_{0.19}Ga_{0.81}N$ layer (Fig. 1, inset). Ohmic contacts are used for source and drain regions, and the gate is a Schottky contact (1.2-eV barrier height). The meshing emphasizes the 2DEG and immediately surrounding layers. The Joule heating density (W/cm^3) is obtained from the simulated electric field and electron density, and using the field-dependent drift velocity.[14] Alternatively, a quasi-2D model was developed predicting HFET dc characteristics and power generation across the gate. The model incorporates Schrödinger–Poisson results for 2DEG density versus gate bias[15] and low-field 2DEG transport results obtained over a limited range of temperatures and carrier densities for our specific device.[5] This model extends into the saturation region with inclusion of a field-velocity expression from Monte Carlo calculations,[16] a "channel length" correction required to accommodate velocity saturation and maintain continuity,[17] and local heating. Above saturation, both methods show the Joule power to be primarily localized to a power peak $\sim 0.1\ \mu$m wide (FWHM, averaged through 2DEG depth) and located in the 2DEG region at the edge of the gate on drain side. A sample FE simulation is shown in Fig. 3(a) for $V_{D-S} = 4$ V ($V_g = 0, P = 1.6$ W/mm). The characteristics of the simulated power peak and the hot-electron processes leading to its formation are consistent with what has been previously described for a GaN HFET.[18] The simulated D–S power density profiles are used directly in our thermal simulation.

For the finite element (FE) thermal analysis[19] we use the same layer architecture inset to Fig. 1. Thermal conductivities (κ) of GaN are known to depend on dislocation density (ρ_D),[20] which varies along the epitaxial growth direction. We divide the GaN layer in our simulation into two layers. The

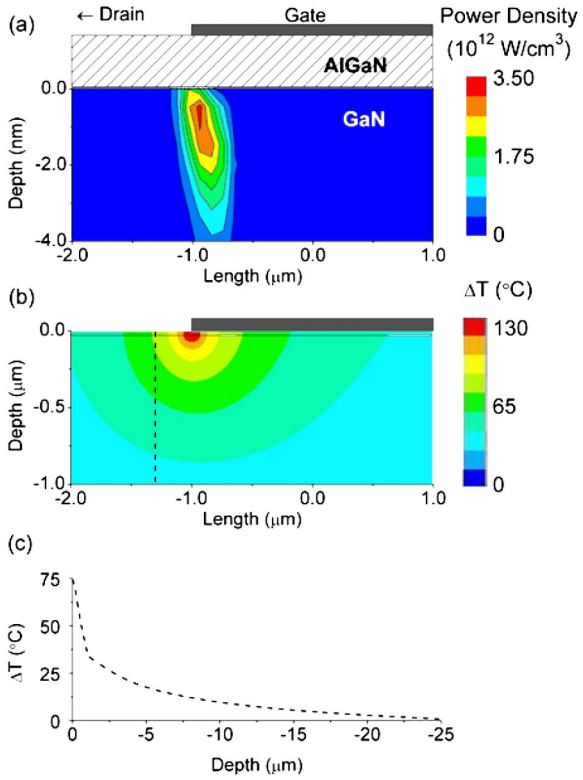

FIG. 3. (Color online) 2D FE simulation of the device at $V_D = +4$ V, source and gate grounded ($P = 1.6$ W/mm): (a) Power density map. AlGaN thickness not to scale; (b) ΔT simulation; (c) ΔT along the vertical line segment (dashed line) shown under the arrow in (b). Note change in units on depth axis between (a) and (b).

first layer is the 150 nm initial growth region, with $\kappa = 1.3$ W/cm K; the remainder of the GaN has $\rho_D < 10^{10}$ cm^{-2} and $\kappa = 1.5$ W/cm K.[20] We take into account the temperature dependence of these values according to Ref. 21. Since the thin AlGaN plays a minor role in dissipating heat, we employ the properties of GaN. We use $\kappa = 4.9$ W/cm K for SiC (Ref. 22) and ignore its temperature dependence, since the observed ΔT rise is small. No thermal boundary resistance[23] is used at the GaN/SiC interface. Heat is generated in the simulation by a thin slab at the AlGaN/GaN boundary according to the lateral dependence of the electrical simulation. Figure 3(b) shows the thermal simulation for the drive conditions of Fig. 3(a). The hotspot is clearly seen near the gate edge. Heat conduction has the expected effect of broadening the hotspot. The vertical line illustrates the micro-Raman probe center. Figure 3(c) shows the simulated ΔT versus depth along the probe line. We see that a significant temperature decrease occurs in the GaN due to the high thermal conductivity of the SiC. For comparison with the measurements, a volume average is calculated from the simulated ΔT across the diameter of the microprobe and along the depth of the device. For the UV excitation, the depth average is taken over d_{opt},[24] while for visible light we average over the full GaN thickness.

Simulations are systematically carried out for several $V_{\text{D–S}}$ values at each V_g studied. Results for ΔT are shown as solid curves in each panel of Fig. 2. We observe distinct heating regions marked by the vertical dashed lines in each panel corresponding to the regions denoted on the I–V dependence in Fig. 1. The low-power range of region I corresponds to the Ohmic regime of the device and approaching the dotted line, the 2DEG becomes depleted at the drain. For $\kappa \sim 1/T$, a quadratic dependence is expected in ΔT versus power across the Ohmic region. The electrical simulations show a gradual increase in the electric field of the hotspot where region I approaches region II. The drift velocity in the hotspot is at its maximum near this boundary. Region II is above saturation, and beyond this point, additional power supplied to the device is dissipated primarily within the hotspot. With the hotspot broadening towards the source[17,18] (i.e., under the gate metal) and the thermal gradient increasing, a diminishing fraction of the hotspot lies within the volume sampled optically. Combined, these factors lead to the slower temperature rise with input power in region II (see Fig. 2). Visible micro-Raman studies on the source side of the device reveal the bulk-GaN ΔT to consistently be $\sim$50% that observed by the drain, thereby confirming the importance of the hotspot. The lateral temperature decrease is also in good agreement with the FE thermal analysis.

Models incorporating the 2DEG, velocity saturation, and thermal effects have provided excellent agreement with measured temperatures for the surface-2DEG, GaN layer, and SiC substrate regions for a range of AlGaN/GaN HFET drive conditions ($V_{\text{D–S}}$ and V_g). We note that the maximum ΔT values measured using UV light are very high in comparison to our visible Raman measurements and those previously reported.[8–10] The simulations project that the *immediate* hotspot region exhibits a much higher temperature than values obtained in the UV studies. For example, under the highest drive power in Fig. 2(b), the simulated hotspot $\Delta T \approx 240$ °C (3.3 W/mm) while the UV and visible measurements give 130 and 55 °C, respectively, thus illustrating the importance of local heating. Our experimental results, backed by simulations, vitally supplement previous work which suggested rather small vertical temperature gradients.[8] Since prior measurements relied solely on lateral mapping by visible Raman, combined with FE analysis, we conclude that depth profiling provides critical information for understanding self-heating in these high-power devices.

The authors at Texas Tech University acknowledge support from the National Science Foundation (ECS-0323640). Sandia is a multiprogram laboratory operated by Sandia Corporation, a Lockheed Martin Company, for the United States Department of Energy National Nuclear Security Administration under Contract No. DE-AC04-94AL85000.

[1] O. Ombacher, B. Foutz, J. Smart, J. R. Shearly, N. G. Weimann, K. Chu, M. Murphy, A. J. Sierakowski, W. J. Schaff, L. F. Eastman, R. Dimitrov, A. Mitchell, and M. Stutzmann, J. Appl. Phys. **87**, 334 (2000).
[2] M. A. Khan, X. Hu, A. Tarakji, G. Simin, J. Yang, R. Gaska, and M. Shur, Appl. Phys. Lett. **77**, 1339 (2000).
[3] M. Singh and J. Singh, J. Appl. Phys. **94**, 2498 (2003).
[4] F. Stengel, S. N. Mohammad, and H. Morkoç, J. Appl. Phys. **80**, 3031 (1996).
[5] S. R. Kurtz, A. A. Allerman, D. Koleske, A. G. Baca, and R. D. Briggs, J. Appl. Phys. **95**, 1888 (2003).
[6] U. V. Bhapkar and M. S. Shur, J. Appl. Phys. **82**, 1649 (1997).
[7] We have established our own phonon shift vs T calibration curves for the HFET GaN and SiC substrate.
[8] M. Kuball, J. M. Hayes, M. J. Uren, T. Martin, J. C. H. Birbeck, R. S. Balmer, and B. T. Hughes, IEEE Electron Device Lett. **23**, 7 (2002).
[9] Y. Ohno, M. Akita, S. Kishimoto, K. Maezawa, and T. Mizutani, Jpn. J. Appl. Phys., Part 2 **41**, L452 (2002).
[10] M. Kuball, S. Rajasingam, A. Sarua, M. J. Uren, T. Martin, B. T. Hughes, K. P. Hilton, and R. S. Balmer, Appl. Phys. Lett. **82**, 124 (2003).
[11] J. Wagner, H. Obloh, M. Kunzer, M. Maier, K. Köhler, and B. Johs, J. Appl. Phys. **89**, 2779 (2001).
[12] APSYS, Crosslight Inc. (2003).
[13] E. M. Azoff, IEEE Trans. Electron Devices **36**, 609 (1989).
[14] K. Seeger, *Semiconductor Physics-An Introduction* (Springer, Berlin, 2004).
[15] F. Sacconi, A. Di Carlo, P. Lugli, and H. Morkoç, IEEE Trans. Electron Devices **48**, 450 (2001).
[16] M. Farahmand, C. Garetto, E. Bellotti, K. F. Brennan, M. Goano, E. Ghillino, G. Ghione, J. D. Albrecht, and P. P. Ruden, IEEE Trans. Electron Devices **48**, 535 (2001).
[17] B.-J. Moon, Y. H. Byun, K. Lee, and M. Shur, IEEE Trans. Electron Devices **37**, 908 (1990).
[18] N. Braga, R. Mickevicius, R. Gaska, X. Hu, M. Shur, M. A. Khan, G. Simin, and J. Yang, J. Appl. Phys. **95**, 6409 (2004).
[19] ANSYS Inc., Release 8.0 (2003).
[20] J. Zou, D. Kotchetkov, A. A. Balandin, D. I. Florescu, and F. H. Pollak, J. Appl. Phys. **92**, 2534 (2002).
[21] E. K. Sichel and J. I. Pankove, J. Phys. Chem. Solids **38**, 330 (1977).
[22] M. E. Levinshtein, S. L. Rumyantsev, and M. Shur, in *Properties of Advanced Semiconductor Materials* (Wiley, New York, 2001).
[23] K. A. Filippov and A. A. Balandin, MRS Internet J. Nitride Semicond. Res. **8**, 1 (2003).
[24] Weighting according to attenuation factor $e^{-(\alpha_{in}+\alpha_{out})z}$ does not produce a significant difference in the simulated ΔT values.